

# Analogical optical modeling of the asymmetric lateral coherence of betatron radiation

B. Paroli,<sup>1,\*</sup> E. Chiadroni,<sup>2</sup> M. Ferrario,<sup>2</sup> and M.A.C. Potenza<sup>1</sup>

<sup>1</sup> *Dipartimento di Fisica, Università degli Studi di Milano and INFN Sezione di Milano - via G. Celoria, 16, 20133 Milano, Italy*

<sup>2</sup> *INFN-LNF - via E. Fermi, 00044 Frascati, Italy*

[\\*bruno.paroli@unimi.it](mailto:bruno.paroli@unimi.it)

**Abstract:** By exploiting analogical optical modeling of the radiation emitted by ultrarelativistic electrons undergoing betatron oscillations, we demonstrate peculiar properties of the spatial coherence through an interferometric method reminiscent of the classical Young's double slit experiment. The expected effects due to the curved trajectory and the broadband emission are accurately reproduced. We show that by properly scaling the fundamental parameters for the wavelength, analogical optical modeling of betatron emission can be realized in many cases of broad interest. Applications to study the feasibility of future experiments and to the characterization of beam diagnostics tools are described.

© 2015 Optical Society of America

**OCIS codes:** (030.1640) Coherence; (340.6720) Synchrotron radiation.

---

## References and links

1. V. Malka, J. Faure, Y. A. Gauduel, E. Lefebvre, A. Rousse, and K. T. Phuoc, "Principles and applications of compact laser-plasma accelerators," *Nat. Phys.* **4**, 447–453 (2008).
2. M. D. Alaimo, M. Anania, M. Artioli, A. Bacci, M. Bellaveglia, F. Ciocci, E. Chiadroni, A. Cianchi, G. Dattoli, G. Di Pirro, M. Ferrario, G. Gatti, L. Giannessi, M. Manfreda, R. Martucci, A. Mostacci, B. Paroli, A. Petralia, V. Petrillo, R. Pompili, M. A. C. Potenza, M. Quattromini, J. Rau, D. Redoglio, A. R. Rossi, L. Serafini, V. Surrenti, A. Torre, C. Vaccarezza, and F. Villa, "Mapping the transverse coherence of the self amplified spontaneous emission of a free-electron laser with the heterodyne speckle method," *Opt. Express* **22**, 30013 (2014).
3. M. D. Alaimo, M. A. C. Potenza, M. Manfreda, G. Geloni, M. Sztucki, T. Narayanan, and M. Giglio, "Probing the transverse coherence of an undulator x-ray beam using brownian particles," *Phys. Rev. Lett.* **103**, 194805 (2009).
4. V. Kohn, I. Snigireva, and A. Snigirev, "Direct measurement of transverse coherence length of hard x rays from interference fringes," *Phys. Rev. Lett.* **85**, 2745 (2000).
5. M. Yabashi, K. Tamasaku, and T. Ishikawa, "Characterization of the transverse coherence of hard synchrotron radiation by intensity interferometry," *Phys. Rev. Lett.* **87**, 140801 (2001).
6. B. Paroli, E. Chiadroni, M. Ferrario, V. Petrillo, M. A. C. Potenza, A. R. Rossi, L. Serafini, and V. Shpakov, "Asymmetric lateral coherence of betatron radiation emitted in laser-driven light sources," *Europhys. Lett.* **111**, 44003 (2015).
7. M. Ferrario, D. Alesini, M. Anania, A. Bacci, M. Bellaveglia, O. Bogdanov, R. Boni, M. Castellano, E. Chiadroni, A. Cianchi, S.B. Dabagov, C. De Martinis, D. Di Giovenale, G. Di Pirro, U. Dosselli, A. Drago, A. Esposito, R. Faccini, A. Gallo, M. Gambaccini, C. Gatti, G. Gatti, A. Ghigo, D. Giulietti, A. Ligidov, P. Londrillo, S. Lupi, A. Mostacci, E. Pace, L. Palumbo, V. Petrillo, R. Pompili, A. R. Rossi, L. Serafini, B. Spataro, P. Tomassini, G. Turchetti, C. Vaccarezza, F. Villa, G. Dattoli, E. Di Palma, and L. Giannessi, "SPARC.LAB present and future," *Nucl. Instr. Meth. Phys. Res. B* **309**, 183–188 (2013).
8. A. R. Rossi, A. Bacci, M. Belleveglia, E. Chiadroni, A. Cianchi, G. Di Pirro, M. Ferrario, A. Gallo, G. Gatti, C. Maroli, A. Mostacci, V. Petrillo, L. Serafini, P. Tomassini, and C. Vaccarezza, "The external-injection experiment at the SPARC.LAB facility," *Nucl. Instr. Meth. Phys. Res. A* **740**, 60–66 (2014).

9. B. Paroli, E. Chiadroni, M. Ferrario, A. Mostacci, V. Petrillo, M. A. C. Potenza, A. R. Rossi, and L. Serafini, "Coherence properties and diagnostics of betatron radiation emitted by an externally-injected electron beam propagating in a plasma channel," *Nucl. Instr. Meth. Phys. Res. B* **355**, 217–220 (2015).
10. J. W. Goodman, *Statistical Optics* (John Wiley & Sons, 2000).
11. M. -C. Chen, P. Arpin, T. Popmintchev, M. Gerrity, B. Zhang, M. Seaberg, D. Popmintchev, M. M. Murnane, and H. C. Kapteyn, "Bright, coherent, ultrafast soft x-ray harmonics spanning the water window from a tabletop light source," *Phys. Rev. Lett.* **105**, 173901 (2010).

## 1. Introduction

The development of radiation sources based upon the emission by ultrarelativistic electrons on curved trajectories has generated great interest in the scientific community. Beam diagnostic tools have been developed along with the sources, in order to verify the expected features of the radiation, to test the applicability for the experiments, to conceive future developments of both the machines and the applications [1].

Soft and hard x-rays are produced by means of bending magnets, wigglers, undulators. The spatial coherence features of radiation can be properly measured in Free Electron Laser (FEL) [2] and undulators with different technique when a quasi-monochromatic condition is obtained. On the contrary the measurement of transverse coherence of radiation produced by sources with a strength parameter  $a_\beta = \gamma r_0 k_b$  needs a monochromator when  $a_\beta \gg 1$  to well distinguish the temporal coherence effects from those of spatial coherence [3–5]. Here  $\gamma$  is the Lorentz factor,  $r_0$  is the oscillation amplitude and  $k_b$  is the oscillation wavenumber. More in general the mutual coherence of radiation should be used to take into account both temporal and spatial coherence effects and it should be considered when the radiation has a broad spectrum. Recently, we have devised particular features of the transverse coherence of broad spectrum radiation emitted by ultrarelativistic electrons undergoing betatron oscillations [6]. We have derived such results on the basis of accurate simulations of the betatron motion of electrons undergoing plasma wakefield acceleration in the SPARC\_LAB source at the National Laboratories of Frascati (LNF) [7]. The simulation has been performed with a hybrid PIC-Fluid code [8], for a low-emittance (2.7 mm mrad) 14 pC electron beam with a 3.5  $\mu\text{m}$  size and 78 MeV initial energy, accelerated in a potential well produced in a  $10^{17} \text{ cm}^{-3}$  dense plasma. The radiated field is obtained by computing the Lienard-Wiechert potentials on a virtual detector [9].

Let the coherence factor be defined as:

$$\gamma_c(\tau) = \frac{|\Gamma(\vec{X}; \vec{X}_0; \tau)|}{[\Gamma(\vec{X}_0; \vec{X}_0; \tau)\Gamma(\vec{X}; \vec{X}; \tau)]^{1/2}} \quad (1)$$

where:

$$\Gamma(\vec{X}; \vec{X}_0; \tau) = \lim_{T \rightarrow \infty} \frac{1}{2T} \int_{-T}^T E(\vec{X}, t + \tau) E^*(\vec{X}_0, t) dt$$

is the correlation function of the electric field  $E$  ( $x$  component). Definition in Eq. (1) is the modulus of the complex degree of coherence. The point  $\vec{X} = (x, y, z)$  is referred to a Cartesian frame with the  $z$ -axis along the average motion of the electron beam,  $\vec{X}_0$  is an off-axis fixed point on the detection plane, which is the reference position for evaluating the coherence and  $\tau = 0$  elsewhere. In [6] we have shown that if the reference point  $\vec{X}_0$  is properly displaced from the average motion axis, the radiation obtained from the numerical simulations shows a characteristic asymmetry. It depends on the elongation and curvature of the particle trajectories, so that it gives statistical information about the dynamics of electrons undergoing oscillatory motions, with direct applications in particle beams and radiation source diagnostics. This peculiar behavior has been given a geometric interpretation in terms of the simultaneous arrival of the emitted field from different positions along the trajectory. On the basis of this interpretation a

simple optical analogy can be found, which shows that this effect has a more general validity and can be applied to several cases of existing sources. Following the optical analogy, we have reproduced the features of a broadband radiation emitted by electrons on a curved trajectory by means of a very simple table top optical setup operating with white light. Coherence measured through a double slit scheme accurately reproduce the expected enlargement effect, thus giving the first experimental confirmation of the effect described in [6]. The feasibility of the experiment is demonstrated also when properly scaled to the radiation wavelength. Therefore, the method presented here and the corresponding data analysis are not only limited to optical sources, but it represents a more general approach for the measurement of the asymmetric properties of coherence up to soft x-rays range. In this sense the results are beneficial and reproduce, through the optical analogy, the coherence properties of betatron radiation. In the following sections we first describe the fundamental interpretation of the asymmetric coherence arising from the curved beam emission, and a discussion of the basic coherence properties is given (Section 2). The optical analogy is then described in Section 3 in terms of general parameters, which make the method applicable on a wide range of real situations. The experimental apparatus and the results obtained with a double slit experiment are reported in Section 4. We finally collect our conclusions and discuss current and future applications of the method.

## 2. Single particle model

A simplified geometrical interpretation of the coherence features described in [6] can be obtained by studying a single particle in a half-cycle of a betatron oscillation. The particle trajectory around the maximum  $x$  elongation is locally approximated by its osculator circle with radius  $R$ . The radiation is instantaneously emitted along the direction of the normalized particle velocity  $\vec{\beta} = \vec{v}/c$ , in a cone of width  $1/\gamma$ .

In Fig. 1, the position of the particle is identified by angle  $\alpha$  at the center of the circle, where  $\alpha = 0$  identifies the osculation point introduced above. Positions  $x(\alpha)$  is the intersection of the emission direction  $\vec{\beta}$  with the observation plane. The geometrical connection between  $P(\alpha)$  and  $x(\alpha)$  is given by the bijection  $x(\alpha) = \tan \alpha (R \sin \alpha - z) + R \cos \alpha$ . The distance between the two points  $P(\alpha)$  and  $x(\alpha)$  is:

$$L(\alpha) = \sqrt{(z - R \sin \alpha)^2 + [R \cos \alpha - x(\alpha)]^2}. \quad (2)$$

The function  $L(\alpha)$  has a minimum in  $\alpha = 0$  for  $z \gg R$  or  $\alpha \ll 1$ . As a consequence, the point  $x(0)$  will receive radiation first. Any other point  $x(\alpha)$  receives light with different delays from the whole trajectory. A position  $x_s$  exists where the radiation from two points with  $\alpha < 0$  and  $\alpha > 0$  will be received simultaneously. Therefore, for a proper fixed point  $\vec{X}_0$  a second peak of the coherence factor is expected. The radiation observed simultaneously from the two points is the origin of the asymmetric enlargement discussed in [6]. The second peak of coherence is related to the particles oscillating in the half plane containing the fixed point. For a single particle case the shape and position of the second peak give information about the electron trajectory. In particular the position of the maximum is expected at about  $-\text{sign}(x_0)(|x_0| - 2r_0)$  (here we consider that the half-cycle of oscillation is in the same half plane of  $x_0$  and  $|x_0| > 2r_0$ ). The decreasing of the coherence factor around the fixed point depends on the value of the derivative  $dL(\alpha)/d\alpha$  that contains the parameters of the trajectory. To observe the first and second peak of coherence the condition  $\Delta L \geq L_c$  is necessary, where

$$\Delta L = |L_0 + c(t_0 - t(0)) - L(0)|,$$

$L_0$  is the optical path from the trajectory to  $x_0$  and  $L_c$  is the coherence length of radiation.  $t(0)$  and  $t_0$  are the emission times at the point  $P(0)$  and  $P_0$ , respectively. When the weaker condition

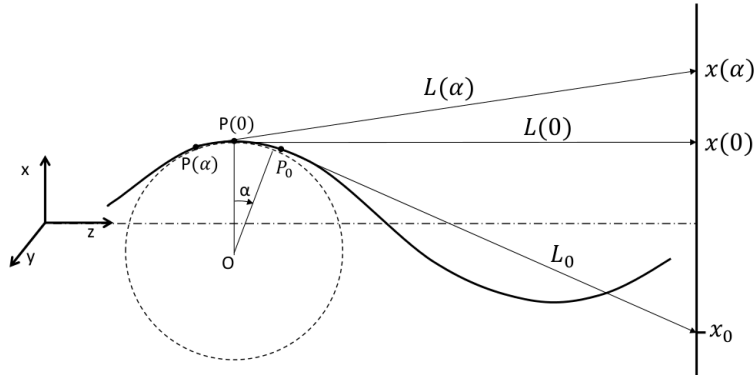


Fig. 1. Sketch of the geometrical interpretation of the asymmetric coherence. Electron trajectory (solid-line) is locally approximated by its osculator circle (dashed-line) at the maximum transversal elongation position. The radiation is observed onto a plane screen transverse to the  $z$  axis.  $x(0)$  receives radiation along the shortest optical path  $L(0)$ . The fixed point position  $x_0$  with its pathlength  $L_0$  are also shown.

$\Delta L \approx L_c$  is satisfied again the additional peaks can be observed. Even if the single particle model adequately describes the observed coherence features, different limitations must be taken into account when an ensemble of particles is considered. In fact the transverse distribution of particles increases the width of the peaks and changes the peak positions. This also limits the possibility of resolving the peaks. The momentum spread of the particles also affects the shape of peaks, while it does not change appreciably their positions. We estimated that a variation of  $\approx 20\%$  of the particle momentum gives a substantial variation of  $\approx 80\%$  in the peak widths and only  $\approx 2\%$  in the peak positions. Moreover, an additional peak will appear on  $\gamma_c$  at the position  $-\text{sign}(x_0)(|x_0| + 2r_0)$  due to the full-cycle of oscillations (as in [6]).

### 3. Anamorphic optical analogy

The geometrical model describing the asymmetric lateral coherence suggests that a similar effect can be rigorously reproduced experimentally by an optical setup with a curved mirror reflecting an incident plane wave. The wave vector  $\vec{k}_r(\alpha')$  of the reflected wave is equal to the wave vector  $\vec{k}_e(\alpha)$  of the radiation emitted by a particle undergoing betatron oscillations, provided that the linear transformation  $\alpha = 2\alpha' - \pi/2$  holds. Here  $\alpha'$  is the angle between the incident radiation and the surface normal of the mirror (at a given reflection point) as sketched in Fig. 2. The optical path from the mirror to the detector is

$$L'(\alpha') = |(z - R \sin \alpha')| \sqrt{1 + \tan^2 (2\alpha' - \pi/2)}.$$

Introducing the function

$$C(\alpha, \alpha') = [(z - R \sin \alpha)^2 - (z - R \sin \alpha')^2](1 + \tan^2 \alpha)$$

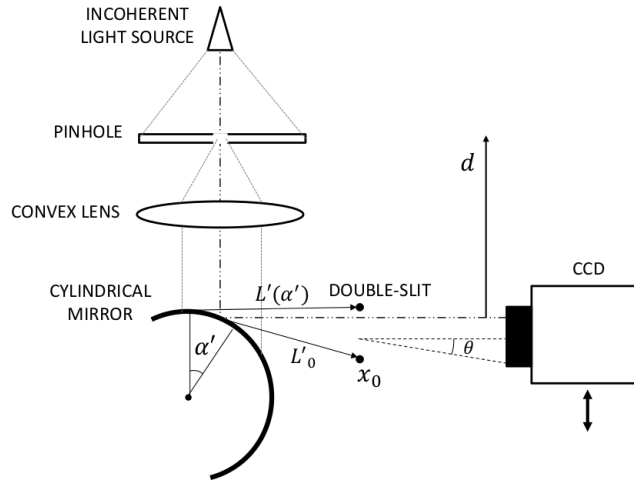


Fig. 2. Sketch of the experimental setup. A collimated radiation illuminates a cylindrical mirror after passing through a 100  $\mu\text{m}$  pinhole. The reflected radiation at different angles  $\alpha'$  will have different optical path ( $L'(\alpha') \approx L(\alpha)$ ) from the mirror surface to the slits. The coherence factor at  $\theta = 0$  is obtained from the interference pattern by using two double-slits with different spacing (250  $\mu\text{m}$  and 500  $\mu\text{m}$ ). We show the position of the fixed point  $x_0$  with respect to the axis  $d$  with its pathlength  $L'_0$ .

we obtain the same optical path of Eq. (2):

$$L(\alpha) = \sqrt{L'^2(\alpha') + C(\alpha, \alpha')}.$$

In the limit  $\alpha \ll 1$  with  $z \geq R$  we obtain

$$C \approx z^2 - [z - R \sin(\pi/4)]^2,$$

while in the limit  $z \gg R$  the function  $C(\alpha, \alpha')$  is negligible and  $L(\alpha) \approx L'(\alpha')$ . Thus the features of the spatial coherence in the case of betatron oscillations and in our optical analogy are just related by a simple linear transformation  $\alpha \rightarrow \alpha'$  on the independent variables. Because the radiation is emitted at different times from each point of the trajectory, the analogy will also take into account different emission times. This analogy is achieved as described below. In the betatron case the trajectory is locally approximated by a circular arc at the time  $t(\alpha) = f^{-1}(t)$  with  $f(t) = \int \beta(t)c/R dt + C$  and  $C$  arbitrary constant. For an almost constant motion around the osculation position,  $t(\alpha) = \alpha R/\beta c + t'$ , where  $t'$  is a constant time. Similarly, within a good approximation a plane wave is reflected from the cylindrical mirror with a linearly-dependent time  $t_{an}(\alpha') = \alpha' R_m/\sqrt{2}c + t''$  around the point  $\alpha' = \pi/4$ , which in our analogy reproduces  $\alpha = 0$ . Here  $t''$  is an initial arbitrary time and  $R_m$  is the mirror radius. Taking  $R_m = 2R\sqrt{2}/\beta$  the time  $t_{an}(\alpha')$  of the radiation reflected from mirror is equal to the time  $t(\alpha)$  of the radiation emitted from the electron beam (except for arbitrarily additive constants).

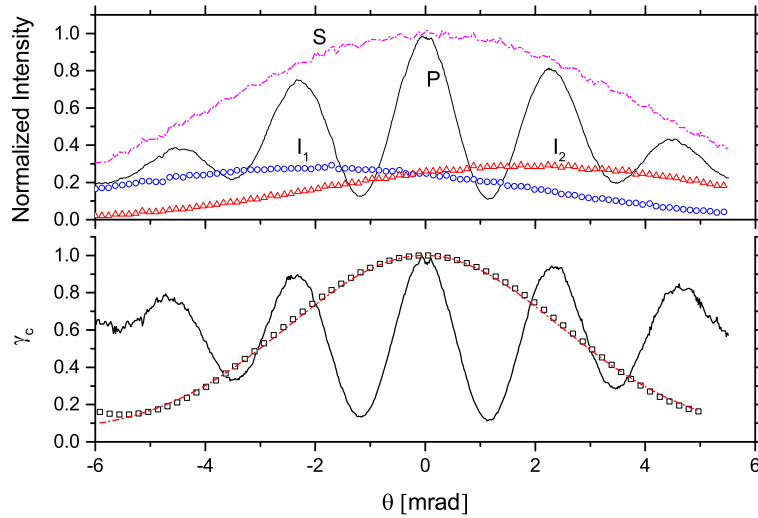


Fig. 3. Top: Normalized interference pattern  $P(\theta)$  and slit intensities  $I_1$  and  $I_2$  measured by using a  $250 \mu\text{m}$  spaced double-slit. Here the center of the double-slit was positioned at  $d = 0$  so that a maximum of the coherence factor is expected at  $\theta = 0$ . Curve  $S$  represents the function  $S(\theta) = (\sqrt{I_1} + \sqrt{I_2})^2$  which is the expected envelop of  $P(\theta)$  as  $\gamma_c = 1$ . Bottom: Coherence factor  $\gamma_c$  extracted from data (squares) using the function  $P/S$  (solid line). The factor  $\gamma_c$  is well approximated with a gaussian function (dashed-line).

#### 4. Experiment and results

The anamorphic optical model has been experimentally realized with a table-top experiment specifically designed to mimic the simulated radiation and to verify its coherence properties. The experimental setup is sketched in Fig. 2. Spatial coherence of a white light source (halogen lamp) is imposed by a  $100 \mu\text{m}$  circular pinhole. The coherence area is about  $1 \text{ mm}$  in size at the surface of a convex lens positioned at a distance of  $150 \text{ mm}$  from the pinhole. Light is then collimated by the lens and sent to a cylindrical mirror with a radius  $R_m = 25 \text{ mm}$ . The reflected radiation is analyzed with two double-slits spaced by  $250 \mu\text{m}$  and  $500 \mu\text{m}$ ,  $70 \mu\text{m}$  wide. The slits are positioned at a distance of  $77 \text{ mm}$  from the mirror along the axis perpendicular to the incident light. The light diffracted from the slits is collected by a Charge Coupled Device at a distance of  $490 \text{ mm}$ , enough for the two diffraction lobes to superimpose. Examples of the interference patterns are represented in Fig. 3 as a function of the angle of observation  $\theta$ . The quantity presented is

$$P(\theta) = I_1(\theta) + I_2(\theta) + 2\sqrt{I_1(\theta)I_2(\theta)}\gamma_c(\theta)\cos(kD\theta),$$

where  $I_1$ ,  $I_2$  are the slit aperture intensities,  $D$  is the slit separation,  $k = 2\pi/\lambda$  and  $\gamma_c$  is the modulus of the complex degree of coherence with  $\tau = 0$  [10].  $\gamma_c = 1$  corresponds to fully coherent fields.  $\gamma_c = 0$  is the condition of completely uncorrelated fields. To verify our model, one slit was fixed at the off-axis position  $d = -250 \mu\text{m}$ , the other slit was moved transversally at positions  $d = -750 \mu\text{m}$ ,  $d = -500 \mu\text{m}$ ,  $d = 0 \mu\text{m}$  and  $d = 250 \mu\text{m}$  and the interference pattern

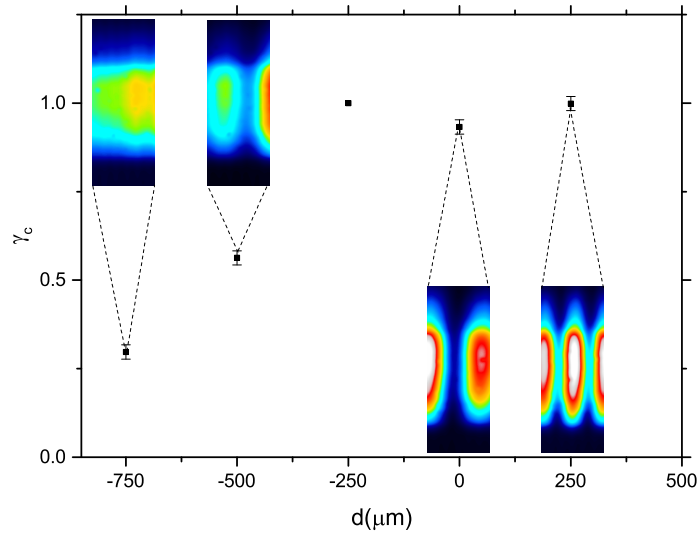


Fig. 4. Coherent factor  $\gamma_c(\theta) = \gamma(0)$  measured around the fixed point at  $d = -250 \mu\text{m}$ . One slit was fixed at  $d = -250 \mu\text{m}$  and the other slit was positioned at  $d = -750 \mu\text{m}$ ,  $d = -500 \mu\text{m}$ ,  $d = 0 \mu\text{m}$  and  $d = 250 \mu\text{m}$ . Images inserts are the measured interference patterns corresponding to the experimental points. The center of the image corresponds to the interference pattern at  $\theta = 0$ . The error bars have been obtained as the maximum error given by slits and CCD positioning.

collected for each position to estimate  $\gamma_c$ . Here  $d$  is the distance of the second slit from the point  $x(0)$ .  $\gamma_c$  has been estimated from the interference pattern, as the amplitude of the gaussian function at  $\theta = 0$ , which shape is shown in Fig. 3. At  $\theta = 0$  the optical paths from the two slits are equals, in agreement with the definition  $\tau = 0$  of Eq. (1). Note that when  $d$  changes, the maximum of the gaussian function (i.e. the maximum of the interference pattern) is not necessarily at  $\theta = 0$ . The value of the gaussian function at  $\theta = 0$  changes in agreement with our model for different values of  $d$ . The experimental data are shown in Fig. 4.

The effects are evident in terms of both  $\gamma_c$  and the interference fringes visibility. The coherence factor decreases rapidly on the left ( $d < -250 \mu\text{m}$ ). A minimum appears at  $x(0)$  ( $d = 0$ ) and a second peak at  $x_s$  ( $d = 250 \mu\text{m}$ ) as expected. These results are in qualitative agreement with both simulations and model. In fact, the maxima position foreseen by the single particle model are  $-250 \mu\text{m}$  and  $250 \mu\text{m}$ , respectively. They are symmetric (with respect to  $d = 0$ ) within a numerical error  $< 0.1 \mu\text{m}$ . It is in agreement with the considered case of a finite width source within an experimental uncertainty of  $d \approx 20 \mu\text{m}$  given by the slits and CCD positioning. As shown in Fig. 4 the values of  $|\gamma_c|$  are compatible with  $|\gamma_c| = 1$  (this value is expected for a single particle) at the maxima position (here the vertical error bars are 0.04). Note that in our optical system we reproduce the first peak as predicted by simulation in [6] accordingly to the anamorphic analogy which reproduces half-cycle of the particle oscillation in betatron motion. The third peak obtained from the simulations has the same physical origin described here, but it is given by radiation emitted by particles oscillating in the opposite half-cycle.

We now discuss the scalability of the experiments with visible light to the betatron radiation

case. In order to resolve the interference pattern, the pixel size  $p_s = 8 \mu\text{m}$  of the detector must be smaller than the spatial period  $p_f$  of the fringes,  $p_f = \lambda z_d / D$  ( $z_d$  is the slit-detector distance). More precisely it should be at least  $p_s \leq \lambda z_d / 2D$ . In our optical setup  $z_d = 490 \text{ mm}$ ,  $\lambda = 500 \text{ nm}$  and  $D = 250 \mu\text{m}$  give  $p_f \approx 120 p_s$ . In the betatron radiation case the detector distance  $z_d$ , the slit separation  $D$  and the slit width  $w$  should be properly scaled to satisfy the condition of above. For example, at a wavelength of  $1 \text{ nm}$ , the condition  $z_d = 2 \text{ m}$  and  $D = 50 \mu\text{m}$  give  $p_f \approx 5 p_s$ . In this particular case the condition  $z \gg R$  is not fully respected since the ratio between the mirror radius and the detector distance is just a factor of 4 and the emulation cannot be performed without taking into account the known correction function  $C(\alpha, \alpha')$ . However for small angles of observation  $\alpha < 100 \mu\text{rad}$  the maxima position predicted by the single particle model are still reproduced, using the analogy, within a systematic error of 10%. The slit separation of  $50 \mu\text{m}$  assumed in this example is again experimentally feasible. On the contrary, the slit aperture must be reduced to ensure that the field overlaps at  $z_d = 2 \text{ m}$  by diffraction. In the Fraunhofer approximation  $z_d \gg \pi w^2 / \lambda$  a slit width  $w$  of a few microns is needed. This makes the measurement actually feasible even with betatron radiation (see for example [11]).

Nevertheless, scaling the setup geometry is still not enough for observing the second peak of coherence. As described above, at least the weaker condition  $\Delta L \approx L_c$  should be satisfied to have the second peak of coherence well distinguished. In the case of the betatron radiation at SPARC.LAB (see [6] for details), the expected temporal coherence length will be in the range  $L_c = 0.5 - 2.5 \text{ nm}$  (here we assume that the setup is not sensitive to photon energies lower than  $1 \text{ keV}$ ). If the double-slit is placed at a distance of  $1 \text{ m}$  from the source and  $R = 0.5 \text{ m}$  we obtain  $\Delta L \approx 1.2 \text{ nm}$ . A displacement of the fixed point of  $50 \mu\text{m}$  (equal to the slit separation) from the axis of average motion of particles has been considered.

An additional limit should be taken into account when the experiment is realized at lower wavelength with a slit separation of hundreds of micrometers. Deformations of few fractions of the wavelength on the mirror could lead to rays deviation at the detector plane up to hundred micrometers. This would lead to an apparent slit separation that is different from the real one sampled on the wavefront. Beyond the limit case should be advantageous to scale the experiment at higher wavelengths. The intensity value at the detector can be also scaled. If the aperture is illuminated by a unit-amplitude normally incident wave of wavelength  $\lambda$ , the maximum intensity of radiation  $I_M$  diffracted by a single slit and detected at a distance  $z_d$  is  $I_M = A^2 / \lambda^2 z_d^2$ , where  $A$  is the area of the aperture. The ratio of the intensities in the x-ray and optical setups is then  $I_X / I_O \approx 320$  (where the same slit length are assumed in calculation and  $w = 5 \mu\text{m}$  is the slit width of the x-ray setup). If the detectors used to acquire the interference patterns have responsivities  $R_X$  and  $R_O$ , the ratio  $I_X / I_O$  multiplied by  $R_X / R_O$  gives an estimation of the ratio between the measured intensities. This permits to perform an experiment also by reproducing the correct fluences of light at the detector, which is important in view of estimating the signal to noise ratios and the actual possibility to extract the information from the experimental data. Our optical analogy is therefore capable to reproduce real conditions encountered in the case of betatron radiation just by simply scaling geometrical parameters defined by the wavelength. Moreover, scaling shows that all the parameters needed to perform the experiment with betatron radiation corresponds to distances, apertures, etc. which are actually feasible, as for example in the double slit experiment with soft x-rays described in [11].

## 5. Conclusions

The optical system designed to reproduce the coherence properties of betatron radiation reproduces the expected behavior of the coherence factor characterized with respect to a fixed point. This peculiar behavior of the coherence has been evidenced on a numerical basis and physically interpreted in [6]. The simplified description has been recalled here to show that a



strong analogy can easily be found with an anamorphic optical system reproducing the fundamental parameters of the radiation emitted by a particle undergoing betatron oscillation. The optical analogical modeling have brought to the first experimental evidence of the behavior described in [6]. Moreover, it extends the validity of the results obtained for that specific case to a much wider class of emission phenomena, which can be advantageously studied in optical experiments finely tuned to represent much more complex emission phenomena at the large scale machines. Works are in progress to exploit the method described here for studying the feasibility and preparing accurate measurements of the coherence properties of radiation emitted by future sources currently under development. Examples are at SPARC\_LAB (Laboratori Nazionali di Frascati) and CERN.

Besides the characterization of the coherence properties of the emitted radiation, we are also exploiting optical analogical modeling like that described here to characterize a diagnostic tool dedicated to a better comprehension of the electron beam properties. The superior simplicity of the optical setup is already giving strong advantages for developing accurate analysis tools in systems currently not yet available for experiments.

In conclusion the possibility to operate with extremely simplified, cheap and flexible systems represents a unique opportunity to work in parallel with the development of new sources, defining the main experimental issues related to the superior complexity of the real ones. Possible applications are in connection with ultrarelativistic beam sources like the third generation synchrotrons where the curvature of particles and the broad spectrum of radiation are imposed by bending magnets or by insertion devices like wigglers.

### **Acknowledgments**

This work was supported by the Italian Ministry for University and Research (MIUR) “FIRB 2012” funds (grant number RBFR12NK5K).